



# A Structural Health Monitoring Technique

S. A. Maqbool, A. Arshad

National University of Sciences and Technology, Islamabad, Pakistan

Received: 06/06/2017

Accepted: 28/08/2017

Published: 17/09/2017

## Abstract

The addition of carbon microfibers has proved to be one of the most effective means of improving the electrical conductivity of cementations matrix. In the present study, 5x5x5cm carbon fiber reinforced mortar specimens were positioned in a 60Hz,  $\pm 2.5V$  AC circuit with a data acquisition system in order to monitor the changes in its electrical resistivity under the influence of different parameters. It was seen that a high fiber fraction and low moisture content makes the specimen act like a pure resistor with negligible capacitance or inductance associated with it. It was also observed that electronic conduction was dominant over electrolytic conduction in a mix proportion with high fiber volume fraction and low water to cement ratio. The resistivity was found to steadily decrease under compressive loading and then increase during the formation of micro and macro-cracks. This study provides an appropriate basis to monitor the health of structures by measuring the increase in electrical resistivity versus the load during the life time of the concrete structures.

**Keywords:** Concrete, carbon fiber, resistivity, loading rate

## 1 Introduction

Structural health monitoring (SHM) is the most modern development in the field of civil engineering. It aims to develop automated systems for the continuous monitoring, inspection, and damage detection of structures. Civil engineering infrastructure is generally the most expensive national investment and asset of any country. In addition, civil engineering structures have long service life compared with other commercial products, and they are costly to maintain and replace once they are erected [1]. Further, there are few prototypes in civil engineering, and each structure leads to be unique in terms of materials, design, and construction. All civil structures age and deteriorate with time. Innovations like fiber-reinforced polymers are being increasingly used to strengthen and repair civil infrastructures. But instead of repairing damages it is wiser to prevent these damages from happening and causing causalities. SHM involves constant monitoring of a structure's condition or change in its condition through smart sensing technologies, which includes the application of fiber optic smart materials, piezoelectric smart materials, self-diagnosing fiber reinforced composites, transmitting device, data acquisition systems and etc. possess very important capabilities of monitoring various physical or chemical parameters related to the health and therefore, durable service life of structures, which make SHM to be an active monitoring system [2,3]. Thus, smart sensing technologies are now currently available, and can be utilized to the SHM of civil engineering structures. Presently various fiber optic smart materials and strain gauges are embedded in the structure to monitor these responses. But with intrinsically smart structural materials there are a number of advantages like, low cost, durability, large sensing

volume, and absence of mechanical property degradation due to the embedding of smart materials, etc [4].

Plain cement mortar is a semiconductor or insulator with resistivity of the very high order. Conductivity of a cement based specimen depends on the pore structure and the chemistry of the pore solution. Introduction of carbon fibers into cementations matrix significantly increases the electrical conductivity enabling one to monitor changes in resistivity under varying degrees of strain [5, 6]. Hence the measurement of variation in resistivity helps one to monitor the response of smart material structures under these varying conditions [7].

This study was carried out to develop an economic smart material using carbon microfibers that can be used in field of civil engineering for the purpose of structural health monitoring. The objective of this research was to develop smart self-sensing cementations matrix for SHM by subjecting it to different loading conditions that exist in field. The results were then examined to propose modifications to make a more effective smart material. Tests were also aimed at determining the best mix proportion for the smart material.

## 2 Materials and Methods

Cement was a Type 1 Ordinary Portland Cement (OPC) obtained from the local market. The chemical composition and properties of the cement used in the study is given in Table 1 and 2, respectively. The locally available, silica fume with bulk density  $550 \text{ kg/m}^3$  were used. The chemical composition of the silica fume used in the study is presented in Table 3. Polyacrylonitrile (PAN) TC-36S 12K based carbon fibers from the nearby industry was used in this study. The properties of PAN are also given in the Table 4.

Two different water reducer i.e. Ultra High Range Sika ViscoCrete-20HE and High Range Sikament 512PK having bulk densities  $1.08 \text{ kg/L}$  and  $1.18 \text{ kg/L}$  respectively were used. Both water reducers were polycarboxylate-based superplasticizer. The sand graded

**Corresponding author:** Arshad Ali, National University of Sciences and Technology, Islamabad, Pakistan, E-mail: [aliarshad08@yahoo.com](mailto:aliarshad08@yahoo.com).

between 0.074-0.5 mm was used for all the samples [8, 9]. The sieve analysis was performed in accordance with ASTM C136-04. Physical properties of sand used, are shown in the Table 5.

Table 1: Percentage chemical composition of OPC used in the study

Chemical composition	Percentage
C <sub>3</sub> S	63
C <sub>2</sub> S	13
C <sub>3</sub> A	6
C <sub>4</sub> AF	11
CaO	65.4
SiO <sub>2</sub>	21.1
Al <sub>2</sub> O <sub>3</sub>	4.44
Fe <sub>2</sub> O <sub>3</sub>	3.68
MgO	0.9
SO <sub>3</sub>	2.7
Loss on ignition	1.16
Alkalies	0.38

Table 2: Properties of OPC used in the study

Laboratory tests	Values	ASTM Specification
Standard consistency	24%	20-26%
Initial setting time	120 min	60 min (minimum)
Final setting time	480 min	375 min (maximum)
Fineness	99%	90% (minimum)
Soundness	5.33 mm	10 mm (maximum)
Specific gravity	3.12	3-3.15

Table 3: Percentage chemical composition of silica fume used in the study

Chemical composition	Percentage
SiO <sub>2</sub>	88.9
Al <sub>2</sub> O <sub>3</sub>	0.0065
TiO <sub>2</sub>	0.002
P <sub>2</sub> O <sub>5</sub>	0.08
CaO	0.93
MgO	0.54
Na <sub>2</sub> O	0.52
Fe <sub>2</sub> O <sub>3</sub>	0.85
K <sub>2</sub> O	0.60
SO <sub>3</sub>	0.25
Loss on ignition	4.5

Table 4: Properties of carbon fiber used in the study

Parameter	Amount
Length	5 mm
Diameter	7 μm
Tensile strength	4900 MPa
Tensile modulus	250 GPa
Elongation	2%
Density	1.81 g/cm <sup>3</sup>

Normal drinking water was used in specimen preparation and their curing. Mix proportions given in Table 6 is the final mix used for making specimens for different sets of experiments, this mix was finalized while aiming for compressive strength above 6000psi,

for that different combination of mixes were used i.e., sand, water/cement ratio, super-plasticizer and silica fumes. Silica fume added at a relatively high dosage in all mixes acted as a dispersant as well as a densifier. Super-plasticizer was added to obtain the desired workability [10].

Table 5: Physical properties of sand used in the study

Physical properties	Amount
Fineness modulus	2.83
Bulk specific gravity	2.65
Bulk specific (oven dry)	2.61
Water absorption	1.5
Apparent specific gravity	2.23

Specimens were casted with dimensions 5x5x5cm. Two copper electrodes of thickness 0.35mm and width 10mm were inserted through the entire depth of the specimen as shown in the Figure 1. The inter-electrode spacing was 3cm. For each experiment a set of nine specimens were casted, three out of them were used for electrical measurements and the graphs were plotted for the average of their results. Rest six specimens were used for compression and split tensile strength. Twenty-four hours after casting, the specimens were carefully demolded and shifted to curing room where electrical measurements were begun. The measurements were made up to an age of 28 days. After each measurement, the specimens were immediately transferred to the curing room [11]. The two-probe resistivity measurement technique was adopted. Electrical resistivity measurements were made by applying a known AC voltage of ±2.5V across the electrodes using a function generator at a frequency of 60Hz [12, 13].

Table 6: Mix proportions by weight of concrete used in the study

Water/cement ratio	Silica fume/cement ratio	Sand/cement ratio	Carbon fiber ratio
0.40	-	-	0
0.40	-	-	1
0.40	0.2	1.5	2
0.40	-	-	3
0.40	-	-	4
0.40	-	-	5

### 3 Results and Discussion

All systems in this universe are in a state of entropy. There are always elements at work that bring about changes in a system. In a system like carbon fiber reinforced cement mortar specimen, there are various factors that play a critical role in changing its resistivity. The following paragraphs enumerate the internal factors that affect the electrical resistivity of such a system.

There are basically two mechanisms of electrical conduction in moist specimens: electronic and electrolytic. Electronic conduction is through the motion of free electrons in the conductive phases, e.g. carbon fibers, and electrolytic conduction is through the motion of ions in the pore solution [14, 15].

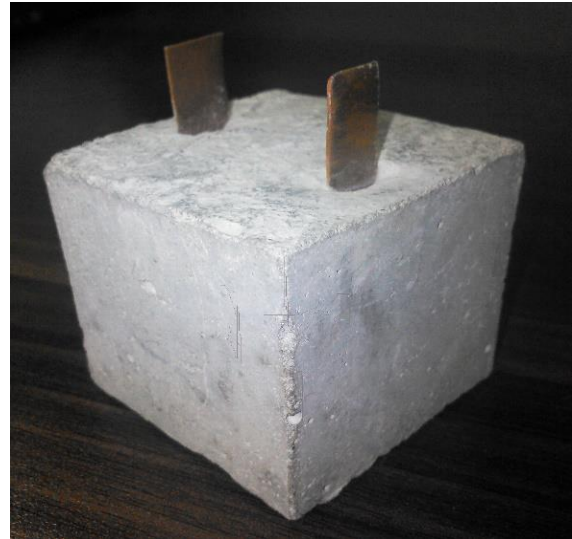
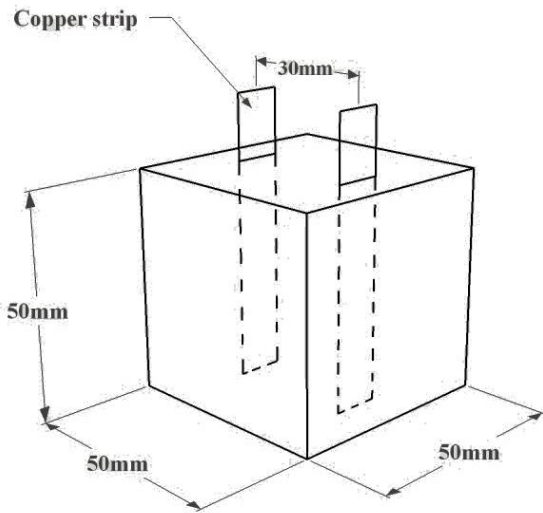


Fig 1: Specimen for resistivity measurements

The conductivity of mortar can be attributed to mainly three media: carbon fibers, the pore solution within the matrix and the physical interface between the fibers and matrix.

Carbon fibers are known to reduce the electrical resistivity of cementations composites. The conductivity of the mix is directly proportional to the volume fraction of carbon fibers and can be visualized as shown in Figure 2. The resistivity behavior for mixes with different fiber fraction volume further asserts this fact as illustrated in Figure 3. The conductivity in a carbon microfiber reinforced mortar specimen follows the phenomena of percolation theory. Percolation theory is basically a geometrical theory that describes the structure of random particles or filaments in a matrix as a function of their volume fraction [16].

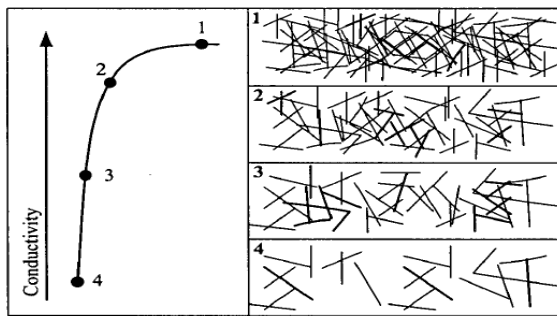


Fig 2.0: Percolation Theory

● 0% CF   ■ 1% CF   ▲ 2% CF

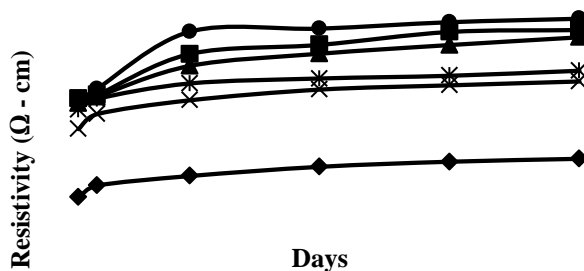


Fig 3: Resistivity as a function of percentage of fiber volume

It postulates that it is only when the volume fraction of the particle or filament exceeds a certain critical value that the particle or filament can come into contact and form clusters. As a result, electrical conduction can occur due to the connection of the clusters. Percolation threshold thus is the critical fraction of lattice points that must be filled in order to create a continuous path of nearest neighbors from one side to another. Thus the electrical conductivity of the specimen also largely depends on the fiber's aspect ratio and material [17]. A higher volume fraction ensures that there exists more fiber-to-fiber contact thus allowing easy passage of current. Moreover a high volume percentage and low w/c ratio makes the specimen act like a pure resistor with negligible capacitance and inductance values. The influence of w/c ratio on the resistivity of mortar is pretty significant. On comparing different combinations of fiber percentage and w/c ratio, it can be seen that the set with 5% volume of carbon fiber and 0.40 w/c ratio offers the least resistance. The combination of 5% fiber volume and 0.6 w/c ratio has lesser resistivity than 5% fiber volume and 0.5 w/c ratio.

This can be attributed to the large amount of pore solution available in the capillary pores of the mix with 0.5 w/c ratio. However the combination of 5% fiber volume and 0.4 w/c ratio has a lesser resistivity value than the one with 0.5 w/c ratio and is lower than even the mix with 0.5 w/c ratio. This is because the former most has larger amount of fines and lesser pores with respect to both the latter ones thus allowing denser packing and more fiber-to-fiber contact [18]. Moreover the large amount of super plasticizer that was added to obtain the desired workability can bring about finer packing of different phases. A lower w/c ratio can also assist in better contact between the electrode and matrix. It can be concluded that on decreasing the w/c ratio from 0.5 to 0.3 the conduction transfers from electrolytic to electronic and fiber-to-fiber contact starts playing a prominent role.

Figure 4 and Figure 5 show the resistivity behavior and drop in voltage of various specimens subjected to compression, respectively.

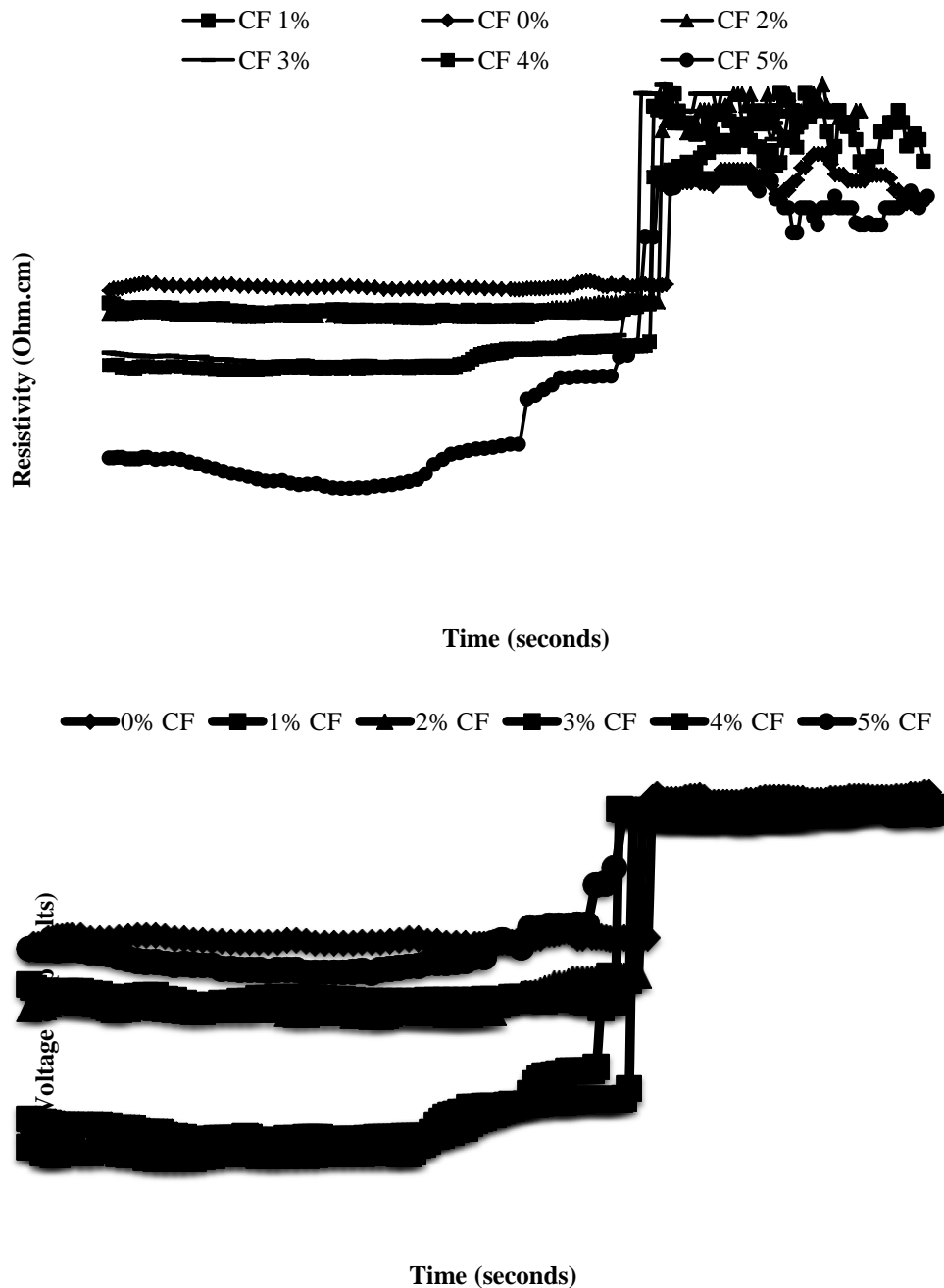


Fig 5: Drop in voltage of various specimens under compression

A significant increase in the maximum strain achieved prior to failure was observed. But the objective of conducting compressive test on smart material is to observe the change in electrical resistivity with increase in load to develop an effective SHM mechanism [19, 20]. All the specimens were loaded till failure at constant loading rate. Initially as load increases for specimen having 0 - 3% carbon fiber no change in resistivity observed which is represented by straight line in graph. Finally as the load reaches the full capacity of the specimen there was a sudden rise in the resistivity value. This can be attributed to the complete failure of the matrix. Although there was a significant decrease in

resistivity of specimen with the introduction of 1 - 3% carbon fibers in the specimen but results are indicating that percolation network was not established resulting in failure to detect any change in electrical resistivity under loading.

As we increase the fiber percentage further to 3 and 4% the resistivity decreases five times of plain matrix. And when placed under compression, initially there was no resistivity change observed but as the load reached 70% of ultimate strength it was seen that the resistivity too started increasing. This increase in the resistivity was a clear sign of formation of micro cracks in matrix. Finally as the load reached the full capacity of the

specimen there was a sudden increase in the resistivity value which shows the complete failure of specimen.

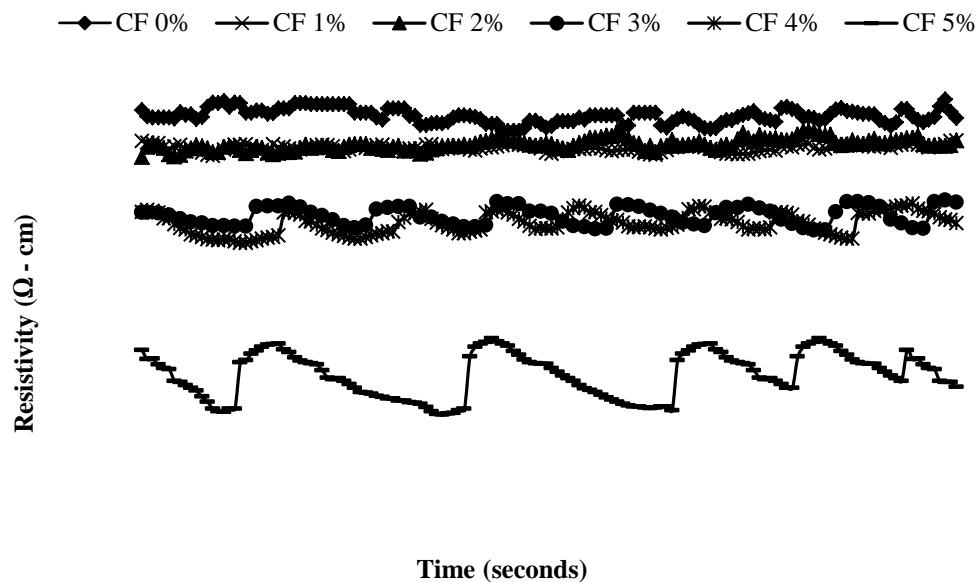


Fig 6: Variation of resistivity under cyclic loading for various specimens

Finally on adding 5% fibers the resistivity decrease 52 times of plain matrix clearly indicating the development of percolation network within the specimens. When placed under the compressive loading, initially as load increases there is a steady fall in the resistivity value. This can be attributed to the increase in contact between carbon fibers by the closing of voids and thus decrease in the distance between the matrix and the copper plates. Then there is a relatively flat portion, which indicates that the closing of original micro cracks and opening of new ones reached a dynamic balance [21, 22]. Gradually as the load increased it was seen that the resistivity too started increasing. This increase in the resistivity was a clear indication of formation of new micro cracks within the matrix, which created distance between the fibers and weakened the fiber-matrix interface. Finally as the load reached the full capacity of the specimen there was a sudden ascends in the resistivity value. This can be attributed to the complete failure of the matrix thus resulting in air pockets within the matrix. The resistivity of air being higher than that of the matrix increases the resistivity of the specimen.

It can be clearly seen from the graph that as the fiber content increases resistivity decreases. Lowest value of resistivity corresponds to the 5% fiber reinforcement. Another important observation was the similar trend of 1% and 2% fiber reinforced mortar samples and same can be observed for 3% and 4% fiber reinforced samples. Samples with 5% fiber reinforcement clearly stand out showing the formation of percolation network. However when used to monitor strain the resistivity changes before the formation of micro cracks are relevant or in other words the resistivity changes that are reversible on load removal are the values that can really tell what is happening in the structure. During the experiment it was noted that the initial resistivity changes only in the range of 5 - 10 % of ultimate load was irreversible. The resistivity changes during load values higher than 10 % of maximum load and up to 45 % of maximum load were

reversible to a great extent. This contradicts to the existing literature [23, 24, 25] where an irreversible change in the resistivity values in the initial phase of loading due to flaw generation was noticed, and then a reversible decrease in the resistivity values till larger cracks was observed. The reason for this could be the low resistivity of the specimen itself, which makes the resistance changes too small to be conveniently detected. From the figures it can be seen that the slope of the resistivity in the elastic range is greater than the slope in the strain hardening and softening regions [26, 27]. Thus, indicating that such a smart material can more efficiently monitor strains in the elastic range of compressive stress application than in the post crack period.

As shown in Figure 6.0, the sensing of damage under increasing stresses was demonstrated in carbon fiber-reinforced mortar. The damage was found to be accompanied by a partially reversible increase in the electrical resistivity of the mortar. The greater the damage, the larger was the resistivity increase. As fiber breakage would have resulted in an irreversible resistivity increase, the damage is probably not due to fiber breakage, but due to partially reversible interface degradation. The interface could be that between fiber and matrix. This behavior was observed within the elastic regime.

In order to study the response of the cyclic loading, samples were cast using different percentage of carbon microfibers. All samples were cured for 28 days before testing. The samples were subjected to cyclic loading. The load during each cycle was gradually increased to 75 % of the ultimate capacity of the sample.

The behavior of the specimen cyclic loading was found to be similar to that under compressive loading. Resistivity decreased in the initial phase till it reached a relatively flat phase after which it increased. An increase in the resistivity towards the end, indicate that micro cracks were beginning to form at higher load values.

Specimens having 0-3% carbon fiber reinforcement

under cyclic loading were unable to observe any significant change in resistivity and data was very noisy for lower fiber (0-3%) content. At a fiber content of 0% by weight of cement, the data was too noisy to be meaningful which can be very clearly seen in the respective figure. This noisy data attributes that at lower carbon fiber percentage no percolation network was formed thus resulting in distorted data.

As we increase the carbon fiber percentage to 3-5% specimen shows significant change in resistance. The stress returned to zero at the end of each loading cycle. The higher the stress, the greater was the extent of resistance decrease. The strain returned to zero at the end of each cycle [28]. The resistance is decreased reversibly upon loading in each cycle. Hence, during loading from zero stress within a cycle, the resistance dropped and then increased sharply on unloading reaching the maximum resistance of specimen. Upon subsequent loading, the resistance decreased and then increased as unloading continued, reaching the maximum resistance of the original resistance at zero stress.

#### 4 Conclusions and Recommendations

The electrical resistivity mortar increases over time. But increase in fiber volume fraction at constant w/c ratio decreased the electrical resistivity significantly. The density of carbon fiber reinforced mortar is reduced due to addition of air voids. A mix proportion with lower w/c ratio and higher fiber volume fraction had lower electrical resistivity and vice-versa. It was found that w/c ratio did not significantly affect the electrical resistivity of samples with higher fiber volume fraction. During compression the elastic range resistivity decreased continuously. On an average, the resistivity changes between 10% and 45% of the ultimate load capacity of the specimen were found to be reversible. The resistance decreases upon compressive strain and increases upon damage. The specimen with higher carbon fiber, were subjected to cyclic loading the samples with higher carbon fiber shows better result, at lower percentage of carbon fiber the results obtained were too noisy and thus making it difficult to make any conclusions.

Further studies can be carried out to study the influence of carbon microfibers on other mechanical properties of mortar such as tensile strength, tensile ductility, flexure toughness, impact resistance and freeze thaw durability etc. Carbon microfiber reinforced matrix can further be used in the field of SHM to study temperature sensing ability, thermoelectric behavior, thermal insulation ability and improved resistance to earthquake.

#### References

1. Harald, S.M., Raphael, B., Jack, S.M. and Michael, H. (2014). Design and properties of sustainable concrete. *Procedia Engineering*, 95, 290-304.
2. Heede, P.V. and Belie, N.D. (2012). Environmental impact and life cycle assessment (LCA) of traditional and 'green' concretes: Literature review and theoretical calculations. *Cement and Concrete Composites*, 34(4), 431-442.
3. Harn, W.K. and Susmita, K. (2014). An attributional and consequential life cycle assessment of substituting concrete with bricks. *Journal of Cleaner Production*, 81, 190-200.
4. Abraham, T., Martin, B., Anicka, A., Chung, Y. and Lasse, R. (2014). Simulation of flash dehydroxylation of clay particle using PROMS: A move towards green concrete. *Energy Procedia*, 61, 556-559.
5. Aldahdooh, M.A., Bunnori, N.M. and Johari, M. (2013). Development of green ultra-high performance fiber reinforced concrete containing ultrafine palm oil fuel ash. *Construction and Building Materials*, 48, 379-389.
6. Megat, M.A.J., Zeyad, A.M., Bunnori, N.M. and Ariffin, K.S. (2012). Engineering and transport properties of high-strength green concrete containing high volume of ultrafine palm oil fuel ash. *Construction and Building Materials*, 30, 281-288.
7. Bisceglie, F., Gigante, E. and Bergonzoni, M. (2014). Utilization of waste Autoclaved Aerated Concrete as lighting material in the structure of a green roof. *Construction and Building Materials*, 69, 351-361.
8. Chen, S.H., Wang, H.Y. and Zhou, J.W. (2013). Investigating the properties of lightweight concrete containing high contents of recycled green building materials. *Construction and Building Materials*, 48, 98-103.
9. Mesci, B. and Eleveli, S. (2012). Recycling of chromite waste for concrete: Full factorial design approach. *International Journal of Environmental Research*, 6(1), 145-150.
10. Payam, S., Hilmi, B.M., Mohd, Z.B.J., Rasel, A. and Syamsul, B. (2014). Structural lightweight aggregate concrete using two types of waste from the palm oil industry as aggregate. *Journal of Cleaner Production*, 80, 187-196.
11. Payam, S., Jumaat, M.Z., Hilmi, B.M. and Johnson, A. (2013). Oil palm shell lightweight concrete containing high volume ground granulated blast furnace slag. *Construction and Building Materials*, 40, 231-238.
12. Qianqian, Z., Xiaoke, W., Peiqiang, H., Wuxing, W., Ruida, L., Yufen, R. and Zhiyun, O. (2014). Quality and seasonal variation of rainwater harvested from concrete, asphalt, ceramic tile and green roofs in Chongqing, China. *Journal of Environmental Management*, 132, 178-187.
13. Salawu, A., Ismail, M., Zaimi, M.A., Majid, Z.A., Abdullah, C. and Jahangir, M. (2014). Green Bambusa Arundinacea leaves extract as a sustainable corrosion inhibitor in steel reinforced concrete. *Journal of Cleaner Production*, 67, 139-146.
14. Chitnis, M.R., Desai, Y.M., Shah, A.H. and Kant, T. (2005). Elastodynamic Green's function for reinforced concrete beams. *International Journal of Solids and Structures*, 42(15), 4414-4435.
15. Corrochano, B.J., Alonso, A. and Rodas, M. (2013). Sequential extraction for evaluating the behavior of selected chemical elements in light weight aggregates manufactured from mining and industrial wastes. *International Journal of Environmental Research*, 7(3), 539-550.
16. Harald, S.M., Michael, H. and Vogel, M. (2014). Assessment of the sustainability potential of concrete and concrete structures considering their environmental impact, performance and lifetime. *Construction and Building Materials*, 67(C), 321-337.

17. James, X. and Masanobu, S. (2013). Rubberized concrete: A green structural material with enhanced energy-dissipation capability. *Construction and Building Materials*, 42, 196-204.
18. Luca, G., Filippo, M. and Marco, A.B. (2011). Assessing environmental impact of green buildings through LCA methods: A comparison between reinforced concrete and wood structures in the European context. *Procedia Engineering*, 21, 1199-1206.
19. Vlastimir, R., Mirjana, M., Snežana, M., Ali, E. and Saed, A.M. (2013). Green recycled aggregate concrete. *Construction and Building Materials*, 47, 1503-1511.
20. Wang, Z.H. and Tan, K.H. (2007). Temperature prediction for contour-insulated concrete-filled CHS subjected to fire using large time green's function solutions. *Journal of Constructional Steel Research*, 63(7), 997-1007.
21. Yu, R., Spiesz, P. and Brouwers, H.J. (2014). Static properties and impact resistance of a green Ultra-High Performance Hybrid Fibre Reinforced Concrete (UHPHFRC): Experiments and modeling. *Construction and Building Materials*, 68, 158-171.
22. Susilorini, M.I.R., Hardjasaputra, H., Tudjono, S., Hapsari, G., Wahyu, S.R., Hadikusumo, G. and Sucto, J. (2014). The advantage of natural polymer modified mortar with seaweed: Green construction material innovation for sustainable concrete. *Procedia Engineering*, 95, 419-425.
23. Zhang, Y., Wei, S., Liu, S., Jiao, C. and Lai, J. (2008). Preparation of C200 green reactive powder concrete and its static-dynamic behaviors. *Cement and Concrete Composites*, 30(9), 831-838.
24. Mahdi, V., Yekkar, M., Shekarchi, M. and Panahi, S. (2014). Environmental assessment of green concrete containing natural zeolite on the global warming index in marine environments. *Journal of Cleaner Production*, 65, 418-423
25. Sheen, Y.N., Wang, H.Y. and Sun, T.H. (2014). Properties of green concrete containing stainless steel oxidizing slag resource materials. *Construction and Building Materials*, 50, 22-27.
26. Zhao, S. and Sun, W. (2014). Nano-mechanical behavior of a green ultra-high performance concrete. *Construction and Building Materials*, 63, 150-160.
27. Arshad, A., Shahid, I., Anwar, U.H.C., Baig, M.N., Khan, S. and Shakir, K. (2014). The wastes utility in concrete. *International Journal of Environmental Research*, 8(4), 1323-1328
28. Bambang, S. (2014). Toward green concrete for better sustainable environment. *Procedia Engineering*, 95, 305-320.